Fabrication of amine cross-linked magnetic biopolymer adsorbent for the removal of a cationic dye and its isotherm, kinetics and thermodynamic study

Md. Masudur Rhaman
Chittagong University of Engineering & Technology (CUET)
Md. Din Islam
Chittagong University of Engineering & Technology (CUET)
Md. Rezaul Karim
Chittagong University of Engineering & Technology (CUET)
Yunus Ahmed
Chittagong University of Engineering & Technology (CUET)
M. K. Mohammad Ziaul Hyder (ziaulhyder@cuet.ac.bd)
Chittagong University of Engineering & Technology (CUET)

Research Article

Keywords: Methylene blue, Wastewater treatment, Jute sticks powder, Cellulose

Posted Date: June 16th, 2022

DOI: https://doi.org/10.21203/rs.3.rs-1742914/v1

Fabrication of amine cross-linked magnetic biopolymer adsorbent for the removal of a cationic dye and its isotherm, kinetics and thermodynamic study

Md. Masudur Rhaman,[a] Md. Din Islam,[a] Md. Rezaul Karim,[a] Yunus Ahmed,[a] M.K. Mohammad Ziaul Hyder,[a,*]

[a] Department of Chemistry, Faculty of Engineering and Technology, Chittagong University of Engineering & Technology (CUET), Chattogram-4349, Bangladesh.

*Corresponding author:
Mobile no: +8801815231060, Email- ziaulhyder@cuet.ac.bd ORCID iD: https://orcid.org/0000-0002-6255-5349

Abstract

A novel amine cross-linked magnetic biopolymer based on jute stick powder (AMB-JSP) was fabricated by in situ chemical co-precipitation method. The adsorbent AMB-JSP was applied to remove methylene blue (MeB) from aqueous solution. The adsorption efficiency of fresh jute sticks powder (JSP) and magnetic jute stick powder (MB-JSP) were also taken in consideration to build up a comparison study with the novel AMB-JSP adsorbent. The maximum MeB removals with AMB-JSP were observed as 85.71% at pH 8.0. Freundlich isotherm was best fitted for AMB-JSP while the Langmuir adsorption isotherm was suited for JSP and MB-JSP. The maximum MeB uptake for JSP, MB-JSP and AMB-JSP were found to be 157.23, 169.45 and 181.49 mgg^{-1}, respectively. The agitation times to reach equilibrium were found to be 160, 120 and 40 min for JSP, MB-JSP and AMB-JSP, respectively at temperature 303.15 K. The interparticle diffusion kinetics showed the best result for JSP, MB-JSP and AMB-JSP. In addition thermodynamic study indicated that the adsorption procedure was endothermic in nature and thus spontaneous. This study reveals that AMB-JSP could be applied as a potential magnetic bioadsorbent for the removal of MeB dye from an aqueous solution.

Keywords: Methylene blue, Wastewater treatment, Jute sticks powder, Cellulose

1. Introduction

Water pollution is a major problem which is principally caused by the toxic substances coming from various anthropogenic activities in water resources such as oceans, rivers, lakes and so on [1] Due to this, the quality of water degrades continuously and becomes contaminated within a short period of time. The contamination of water can happen in a number of ways [2]. Dyes are one of the major pollutants coming from various industries such as textile, paper and plastic industries and are responsible for the pollution of a major portion of water [3]. Therefore, significant considerations should be taken to handle the effluent containing dyes before release from these industries. Methylthioninium chloride is well known as methylene blue (MeB) is used as organic cationic dye and medication [4]. It is used in various applications such as wool or cotton or silk dying purposes, dyeing of leather, coloring of plastics and paper, producing paints and ink for printing purposes. Furthermore, it also has a significant impact for the treatment of infection caused by fungi and the load of microbes in milk [5]. Apart from the usefulness of this dye, it is responsible for various adverse effects on the health of human being for instance aching head pain, hypertension, rapid heartbeat or palpitations, nausea, diarrhea, vomiting, cyanosis, shortness of breath (dyspnea), jerky movements of the arms, legs, body, or head, fever, trouble seeing, lightheadedness or feeling faint, abnormal or incoherent speech, and cancer [6]. For this reason, MeB should be removed from the waste water coming with the effluent from various industries. The removal of MeB is difficult because of its atomic structure, stability, oxidation reaction, high visibility in light and properties like xenobiotic compounds [7]. The elimination of MeB from effluent has been broadly studied for decades, and numerous methods have been established, including degradation of carbon skeleton with oxidation, biochemical and photocatalytic reaction, electrocoagulation, and adsorption [3]. Among these techniques, adsorption is the most promising, recognized and cost-effective methods for the removal of MeB and other pollutants as a result of it is economical, highly efficient, convenient in operation, and recyclable properties [8, 9]. Agricultural waste materials are the most effective biopolymers among all other adsorbents. In recent decades, a huge number or range of modified and non-modified biopolymers such as magnetic peanut husk [10], tea waste [5], citrate modified bagasse [5], biologically activated banana peel, garlic peel[11], *Lathyrus sativus* husk [12], pineapple waste [13], polydopamine functionalized recyclable coconut shell [14], magnetic coffee husk hydrochar [15], carbonaceous hydrocarbon from coffee husk [16], walnut shell powder [17], rice husk [18], magnetic alginate/rice husk bio-composite [19], fava bean peel [20], soybean hulls [21], silica nanoparticle extracted from skewer coconut leaves[22], crab shell chitosan/neem leaf composite [23], neem leaf powder (NLP) and activated NLP [24], pine cone biomass of *Pinus radiate* [25], activated carbon from Palm Fibres [26], $ZnCl_2$ activated carbon from wood apple outer shell [27], brown linseed reoiled cake-activated carbon [6], modified bamboo hydrochar [28] and magnetized papaya seeds [29] have been applied for the removal of MeB from

aqueous solution. It is necessary to find an adsorbent material that is available abundantly and low-cost [30]. In Bangladesh jute is known as the golden fiber and its average production is 1.09 million tons/year. Jute fiber is widely used in the preparation of clothes, bags, tobacco sheets and other decorative items. Jute stick is obtained after the separation of jute fiber which doesn't have significant economic value but low-grade fuel in household cooking. It has been observed that biopolymer derived from different parts of jute plants is effective for the removal of MeB, such as jute fiber carbon [31], ZnO/biochar nanocomposites from jute fibers, jute stick charcoal [32] but the application of JSP for the removal MeB has not been done yet. The removal of JSP after adsorption of MeB from solution is the major challenge because the treated water might be contaminated due to the presence of JSP. For this reason, an effective separation technique is required. Therefore, the raw JSP is modified with magnetic Fe_3O_4 which gives magnetic properties to the adsorbents and by using a small magnet; the separation can be done from the effluents after treatment. In our previous work, we have synthesized the MB-JSP which was used for the removal of hexavalent Cr(VI) from wastewater [33]. In this study, the MB-JSP is modified with amine crosslinking to produce the novel amine cross-linked magnetic biopolymer based on jute stick powder, AMB-JSP. The physicochemical characteristics of JSP, MB-JSP and AMB-JSP have been determined by FESEM, VSM, XRD, FTIR and TGA. After that the effects of adsorbent dosage, pH, temperature, contact time and regeneration efficiency were also assessed. Besides, the results of the experiment were assessed via the pseudo-first-order, pseudo-second-order and intraparticle models. We also compare the adsorption capacities, mode of adsorption and kinetics of AMB-JSP with the raw JSP and MB-JSP.

2. Material and Methods

2.1. Bio adsorbent and Reagents

The bio-absorbent was collected from Kustia District under Khulna Division of Bangladesh. At first the raw jute sticks were dried in the oven for 3 hours at 100^{o}C followed by washing with deionized water and was crushed into a primary crusher. Then the crushed jute stick was dried in the sun and made into 20∼500 μm particle size through roll crusher and hammer mills. All of the chemicals like $FeSO_4.7H_2O$, $FeCl_3.6H_2O$, $NH_3.H_2O$, NaOH, $K_2Cr_2O_7$, HCl, KCl, NaCl, diphenyl carbazide, epichlorohydrin, ethylenediamine, triethylamine, and N, N-dimethylformamide were purchased from Sigma Aldrich.

2.2. Synthesis of amine cross-linked magnetic biopolymer-based jute sticks powder

In situ chemical co-precipitation technique through some modification was applied to prepare the amine-cross-linked magnetic bio adsorbent based jute stick powder (AMB-JSP) [34]. Firstly, in 1000 mL conical flask 250 mL deionized water, 13.9 g (0.05 molL^{-1}), and 27.028 g (0.100 molL^{-1}) $FeCl_3.6H_2O$ (1:2) were added. After that 350 mL suspension with $Fe^{2+}$and Fe^{3+} was made by adding 8.0 g of virgin jute stick powder (JSP) by stirring in

a magnetic stirrer at 350 rpm at 80°C for 40 minutes. To avoid oxidation the inert atmosphere was created by passing N_2 gas. Then the solution of NH_4OH (25%) with a volume of 100 mL was taken slowly to observe the black color and then set the mixer to stir with 300 rpm at 80°C. Then, after6 h of stirring, the products gained from this method were cleaned sensibly by using deionized water. After that, the magnetic bio adsorbent based on jute stick powder (MB-JSP) was obtained. Then, the MB-JSP was dried in a vacuum oven at 85°C for 5 h.In the further process, the reaction between MB-JSP, N, N- dimethylformamide (20 mL) and epichlorohydrin (20 mL) took place and stirred at 300 rpm for 1.5 h at 85°C. Then the reaction mixture was stirred for 1h at 300 rpm with the addition of 6 mL ethylenediamine along with 25 mL of triethylamine. Lastly, the products were obtained from keeping them overnight drying at 105°C and named amine crosslinked magnetic biopolymer-based jute stick powder (AMB-JSP).

2.3. Preparation of Stock solution of Methylene Blue

A synthetic MeB adsorbent was used in analytical grade without further purification. 1 g of MeB was dissolved in one liter of water to produce stock solution and its pH was maintained by addition of 0.1 M HCl or 0.1 M NaOH..The dye solution was then diluted by using deionized water to afford the suitable range of concentration of investigated solutions. By using a UV-visible spectrometer,the residual dye concentration was determined at λmax = 668 nm by taking different samples at certain time intervals and the supernatant obtained by centrifuge was studied for the MeB residue. A calibration curve of the MeB solution was then plotted between concentration and absorbance.

2.4. Measurement of Physicochemical Characteristics of JSP, MB-JSP and AMB-JSP

The adsorbent morphology was determined by Field Emission Scanning Electron Microscope (FESEM) with EDX attachment (Model: JSM 7600F, JEOL, Origin: Japan). A vibrating sample magnetometer (VSM, Model: LDJ9500, Origin: Germany) was accustomed to maintain the magnetic actions of particles at room temperature. To determine the structural properties of MB-JSP XRD Diffractometer (Model: Empyrean, PANalytical, Origin: United Kingdom) (Cu-K radiation at 40 mA and 40 kV) was used. The functional groups of the bio adsorbents were examined by means of FTIR (Model: IRTracer-100, Origin: Japan) within the range from 400 to 4000 cm^{-1}.A simultaneous thermal analyzer (Model: NETZSCH STA 449F3, Origin: Germany) was used to estimate the thermo gravimetric (60 $mLmin^{-1}$) at rate of 26°C/10.0 ($Kmin^{-1}$), and the temperature was maintained sensibly at 25 to 800°C. With a phase size of 0.001°C and rapidity of scan 0.5 s per stage, outcomes were collected in the range of 10to 80°C and a rapidity of scan was 0.5 s per step.

2.5. Batch adsorption experiment by JSP, MB-JSP and AMB-JSP

The batch experiments of known quantities of the JSP, MB-JSP and AMB-JSP biopolymers through 50 mL of MeB solutions of exact concentration in a sequence of 250 mL conical flasks were used to measure the adsorption measurement. Then the resulting mixture was shacked in a water bath at constant temperature at 30°C by 120 rpm for 240 min. After the completeness of shaking the reaction mixtures were centrifuged and a UV spectrometer was used to check the residual dye concentration. The experiment was done by changing the various conditions of reaction mixture such as pH, agitation time, temperature, adsorbent dose, and initial concentration of MeB as a part of adsorption isotherm and adsorption kinetics. The total number of adsorbed MeB onto the surface of JSP, MB-JSP, AMB-JSP was determined through the following equation:

$$q_t = (C_O - C_t)/mV \quad (1)$$

Where, Co = initial dye concentration (mgL^{-1}),

C_t = concentration of dye at any time t,

V = volume of solution (L) and

m = *mass* of pine cone powder in (g).

The % of dye removal was determined by-

$$\%\, removal = \{(C_O - C_t)/C_t\} \times 100 \quad (2)$$

All quantities are in general reproducible within ± 10%. To compare the amount of adsorption qt (mgg^{-1}) and extent of adsorption % between the raw and chemically modified JSP, the same experiments were repeated for MB-JSP and AMB-JSP**.**

2.6. Regeneration experiment

By a batch technique, the renewal processes of adsorbents (JSP, MB-JSP, and AMB-JSP) along with the recovery of the remaining chemicals are substantial and are done with several types of chemical agents. The adsorbent with MeB was engaged in the appropriate chemical environment for desorption and then strongly stirred at 300 rpm at room temperature for 2 h. The ratio of elution was determined by the amount of MeB adsorbed on the adsorbent particles.

3. Results and discussions

3.1. Characterization of adsorbents

The functional groups of the modified adsorbent were determined by FTIR over the range of 4000-400 cm^{-1} in Fig 1. FTIR spectra of JSP, MB-JSP, and AMB-JSP showed strong bands at 3397 cm^{-1}, 3379 cm^{-1}, and 3409 cm^{-1}indicating the presence of N-H stretching. The band at 2909 cm^{-1}, 2901 cm^{-1}, and 2906 cm^{-1} indicating C-H stretching. Those at 1642 cm^{-1}, 1612 cm^{-1}, and 1638 cm^{-1} are due to the bending vibration of N-H. The peaks at

625 cm^{-1} and 625 cm^{-1} are the characteristic peaks of MB-JSP, and AMB-JSP denoted the modification of the adsorbent by Fe_3O_4.

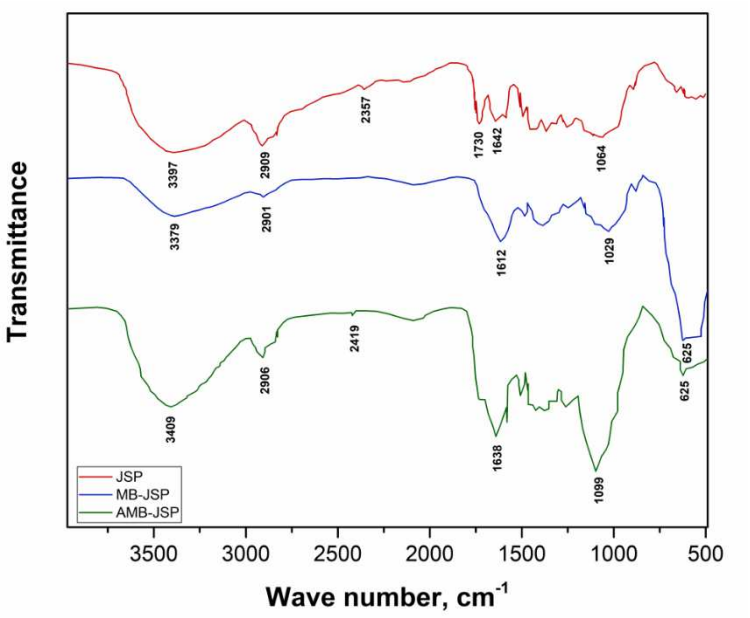

Fig 1. FTIR spectra of JSP, MB-JSP & AMB-JSP before the MeB adsorption

XRD (X-ray powder diffraction), is a tool for phase identification of the crystalline material and provides information on unit cell dimensions. The material to be analyzed was excellently grounded, homogenized, and bulk composition of this was studied. X-ray diffraction (XRD) patterns of JSP, AMB-JSP and Fe_3O_4 were shown in Fig 2.

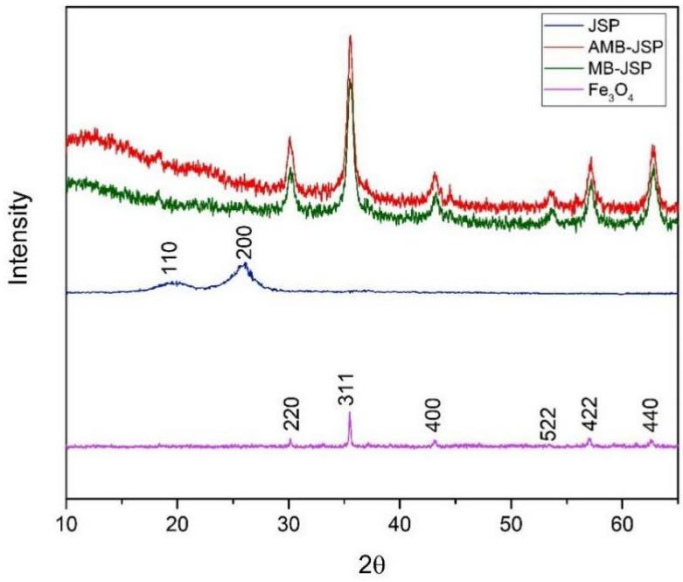

Fig 2. XRD pattern study for the identification of crystalline structures of JSP, AMB-JSP, MB-JSP and Fe_3O_4.

The lattice structure of Fe_3O_4 was confirmed by diffraction peaks of the composites (30.1°, 35.4°, 43.0°, 53.45°, 56.9° and 62.5°) indicating to planes at (2 2 0), (3 1 1), (4 0 0), (5 1 1), (422), (4 4 0) respectively. As compared with the XRD pattern of JSP, the peaks of 17.61° and 25.2° were distinguished which were not present in both MB-JSP and AMB-JSP, providing the crystallinity of cellulose that was not detected for MB-JSP and AMB-JSP. These revealed that the JSP crystalline structure has been dilapidated throughout preparation.

Scanning electron microscope (SEM) is used to investigate the basic physical properties and surface morphology of the adsorbent. SEM images of raw JSP, MB-JSP and AMB-JSP are illustrated in Fig S1. By comparing with the bare surface of the JSP, the surface pore channels were increased dramatically in MB-JSP and AMB-JSP. In addition, the particle size of the MB-JSP and AMB-JSP were reduced to nano size approximately 10-100 nm from the micrometer sized JSP. This reduced size was responsible for the increase of surface area and pore volume which increased the enhanced adsorption rate of MeB by MB-JSP and AMB-JSP.
In Fig. S2, the compositions of elements present in AMB-JSP are shown by the EDX investigation. The presence of significant amounts of C, N, Fe and O (38.32, 3.29, 30.00, and 26.29 mass%) clearly reveal the presence of Fe_3O_4 and $-NH_2$ in synthesized AMB-JSP.
The magnetic hysteresis loop is used for identification of the response ability of magnetic materials. It is seen in Fig. S3, the saturation magnetization of AMB-JSP was 9.60 emu/g suggesting enough magnetic properties to separate AMB-JSP from aqueous solution. In addition, no pronounced hysteresis was found in AMB-JSP which showed retentivity and coercivity of adsorbents was almost zero. The magnetization of AMB-JSP allowed them to separate easily from the treated solution and collected them using an external magnet within 10s.

Thermal analysis of JSP and AMB-JSP showed three stages of mass lossand MB-JSP showed four stages of mass loss at the ranges of different temperature from 25 to 800°C illustrated in Fig S4. For AMB-JSP, the mass loss was alienated into three major steps. The initial period reached at 30–200°C with a mass loss of 8.00~10.00% indicating release of moisture and low molecular weight volatile compounds. Then, the mass loss of the second stage reached 200 to 300°C revealed the decline of samples due to destruction of lignocellulosic structures and dehydration of hydroxyl groups present on the structure. The main pyrolysis process occurred when the temperature rose 300 to 800°C. After this period, loose porous char was formed when the weight loss of samples reached 55% with the release of various volatile components.

DSC curves of JSP, MB-JSP and AMB-JSP are also shown in Fig S4. Endothermic reaction occurred due to the gas molecules volatilization whereas the production of charring is responsible for the exothermic reaction (solid residue). For MB-JSP, the removal of moisture by evaporation was attained at 92°C. Then a slight exothermic peak achieved which was accountable for the decomposition of hemicellulose and lignin at 340°C. Finally,

owing to formation of char and the magnetic part of AMB-JSP a significant exothermic peak was found at 400-500°C.

3.2. Batch adsorption study of methylene blue

3.2.1. pH Effect on the removal MeB

The effect of pH for the MeB removal with synthesized adsorbents is illustrated on Fig. 3.The removal percentage of MeB increased with the increase of pH and it reached at maximum about 95 mgL^{-1} at pH 6.0 by using JSP as an adsorbent. The pH effect on MB-JSP adsorbent also showed a rising trend with the increase of pH value and around 88 mgL^{-1} of MeB removed at the pH value of 7.0. For AMB-JSP, the maximum value of MeB removal percentage was about 85 mgL^{-1} at pH 8.0. It was reported that the surface of adsorbents covered by H^+ ions present in the solution at lower pH increases the positive charges on this surface [35]. This positive charge could not allow the cationic dyes to get attached on the surface due to the electrostatic repulsion. On the other hand, higher pH provides a large number of OH^- ions which makes the surface negatively charged. As a result, the cationic dyes easily attach on the negatively charged surface due to electrostatic force of attraction. At lower pH, the surface of JSP is covered by positive H^+ ions which repulse the cationic MeB dye. Due to this the initial removal percentage by JSP was minimum value. With the increase of pH, the number of OH^- ions in the solution increases on the surface of JSP which attracts more cationic MeB dyes by electrostatic force of attraction. After reaching the maximum value, the removal percentage remained close to the maximum value because of the presence of enough dye molecules on the surface which did not allow further adsorption. In case of MB-JSP and AMB-JSP,the Fe_3O_4 and NH_2 groups blocked the available OH^- groups on the surface of raw JSP, as a result the maximum removal percentage of MeB was obtained at pH 7.0 and 8.0 respectively as compared to the pH value of raw JSP.

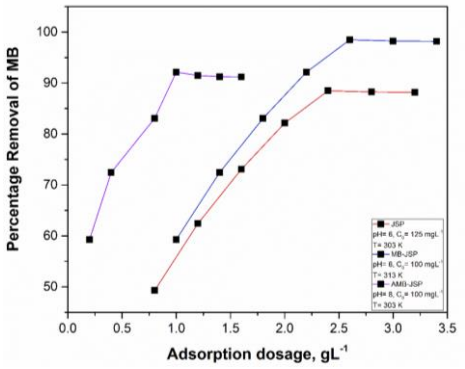

Fig 3. The effect of pH on MeB removal by JSP, MB-JSP and AMB-JSP

3.2.3. Effect of temperature with different initial concentration

The effect of temperature on the adsorption of MeB at different initial concentrations is shown in Fig. S5. At temperature 40°C or 313.15 K, both JSP and MB-JSP gave the maximum percentage of MeB removal 76.63 and 84.14 at the initial concentration of 25 mgL^{-1} for both cases.

The result from our study revealed that the adsorption rate improved with the increase of temperature which specified the process was endothermic in nature. On the other hand, the AMB-JSP also showed the raising trend of removal percentage which also represented the process was endothermic. At temperature 303.15 K, AMB-JSP gives the maximum percentage of MeB removal 85.44 at the initial concentration of 25 mgL^{-1}. In comparison with JSP and MB-JSP, the maximum percentage of removal of MeB removal was obtained at a lower temperature which is due to the presence of an amine functional group in AMB-JSP.

3.2.4. Effect of agitation time with different initial concentration

In this study, the effect of agitation time on the removal of MeB for the JSP, MB-JSP and AMB-JSP biopolymers is illustrated in Fig. S6. For JSP and MB-JSP, the maximum percentage of the MeB removal was obtained in agitation time 160 and 120 min at the equilibrium pH 6 at temperature 303.15K respectively.

On the other hand, the removal percentage of MeB was maximum in agitation time at 40 min where the equilibrium pH 8.0, temperature 303.15 K and absorption dose of 1 gL^{-1}. From the observation of our research work, it was concluded that with the increase of time there was no obvious rise of adsorption as the active sites present on the surface of our adsorbents became saturated. Therefore, a repulsive force was generated between the adsorbent and adsorbate which was the main reason for the almost constant removal rate of MeB.

3.2.5 Adsorption isotherms

The contact mood of adsorbent with the MeB is determined by using adsorption isotherm which created a connection between the MeB ions in solution and number of MeB ions in the solid surface that both phases exist at equilibrium position.The adsorption isotherm of Langmuir, Freundlich and Temkin have been studied and their adsorption isotherm shown in Fig. 4, Fig. 5, and Fig. 6 for JSP, MB-JSP and AMB-JSP, respectively.

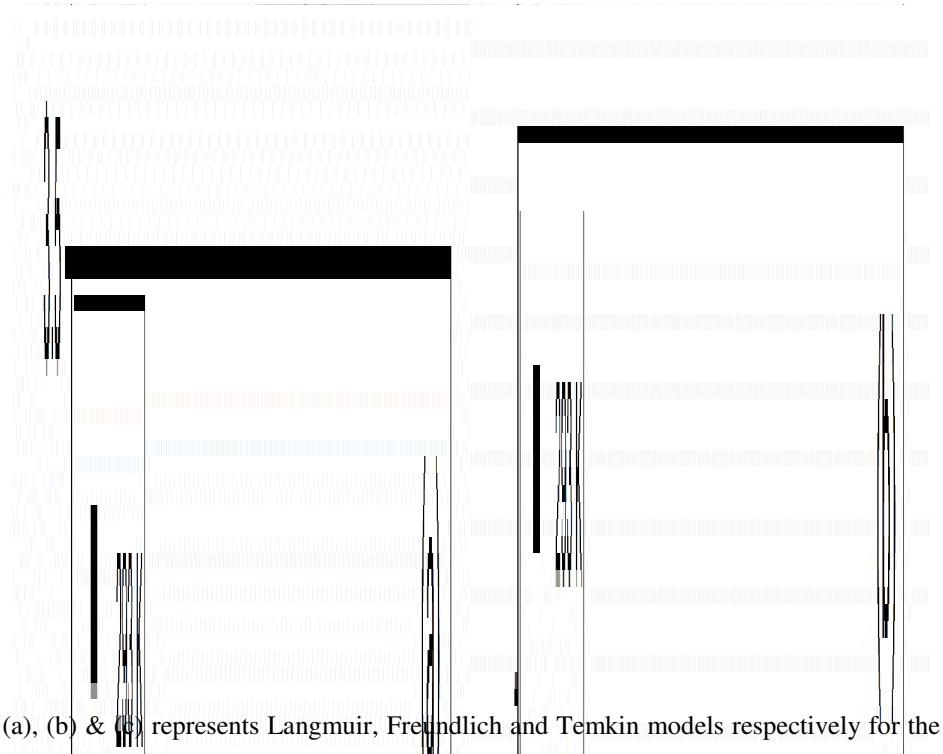

Fig 4. (a), (b) & (c) represents Langmuir, Freundlich and Temkin models respectively for the MeB removal by JSP

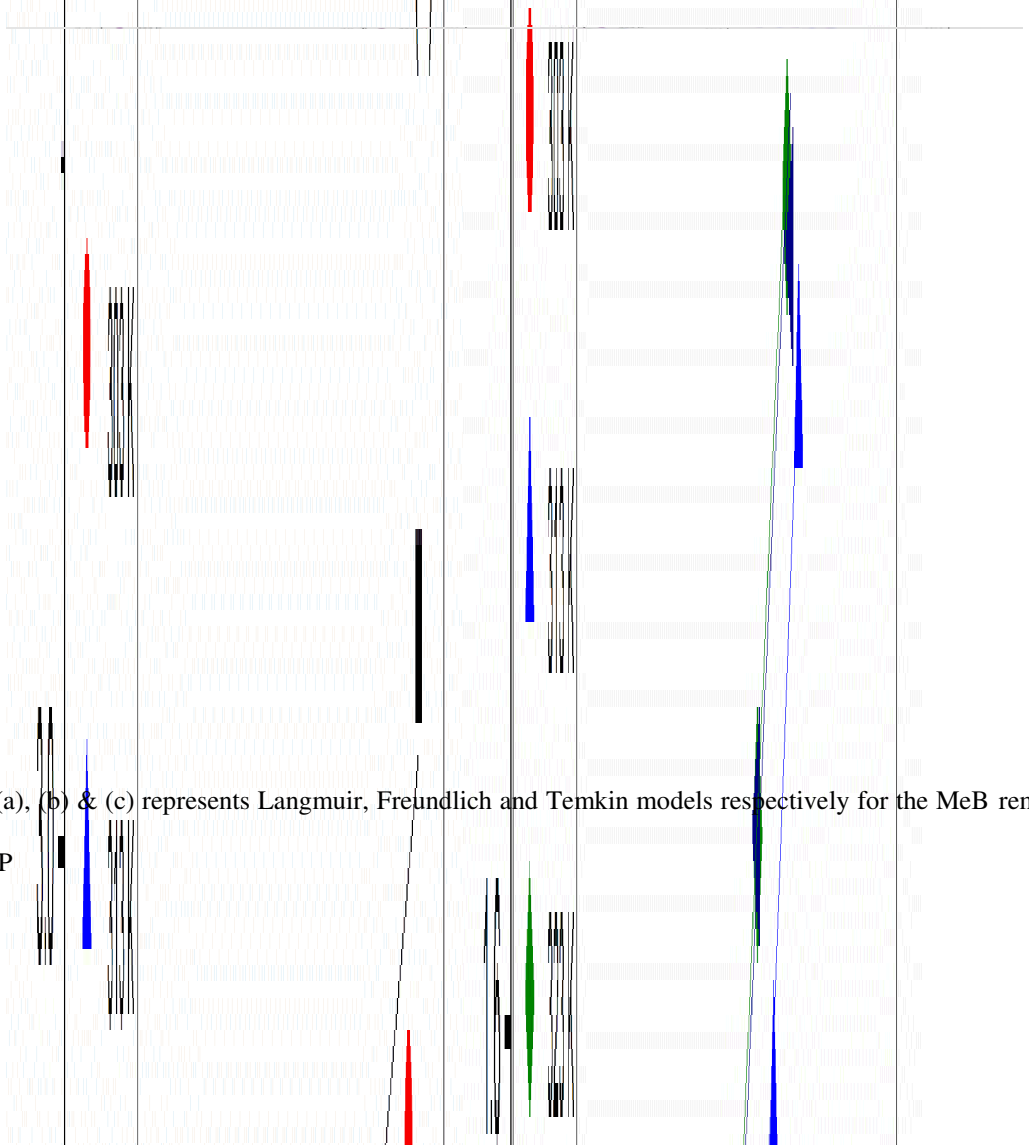

Fig 5. (a), (b) & (c) represents Langmuir, Freundlich and Temkin models respectively for the MeB removal by MB-JSP

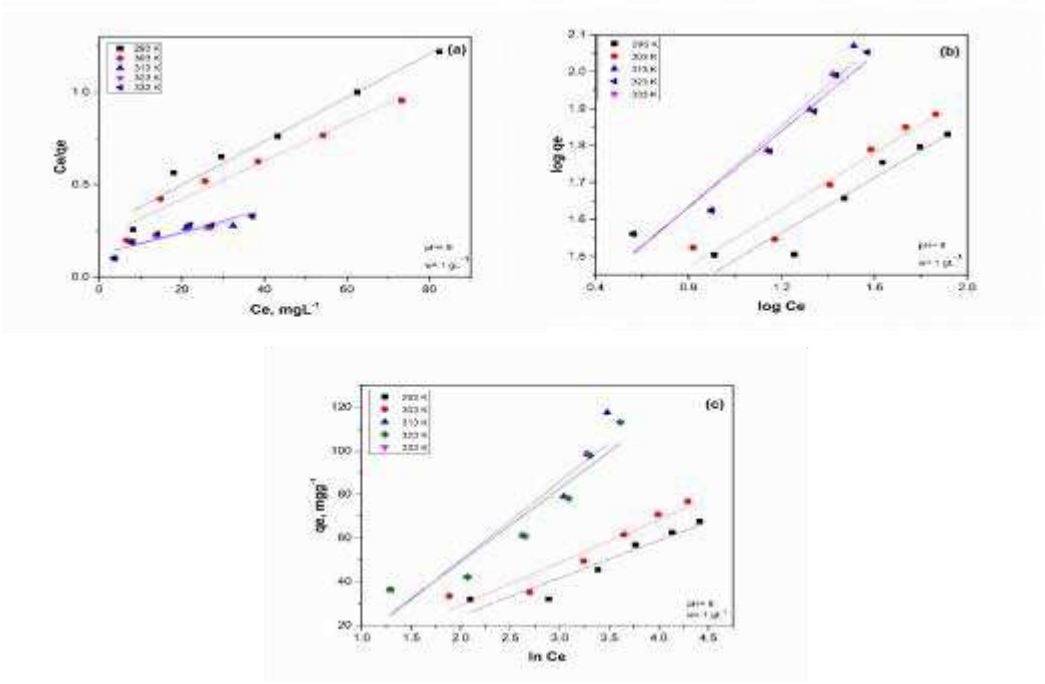

Fig 6. (a), (b) & (c) represents Langmuir, Freundlich and Temkin models respectively for the MeB removal by AMB-JSP

According to Langmuir a unimolecular thick adsorbed layer is generated on the adsorbent surface and there is no significant interaction between the adsorbent and adsorbed molecules. The Langmuir adsorption isotherm stood

$$q_e = (q_m - K_L C_e)/(1 + K_L C_e) \quad (3)$$

Converting the equation into linear form as

$$1/q_e = 1/q_m + 1/q_m K_L C_e \quad (4)$$

Here, C_e (mgL^{-1}) = concentration of MeBat equilibrium,

q_e (mgg^{-1}) = adsorbed quantity of MeB

q_m(mgg^{-1}) = adsorbent maximum efficiency and

K_L (Lmg^{-1}) = equilibrium constant.

Freundlich adsorption isotherm stated that the variation in the amount of matter adsorbed by a unit mass of solid adsorbent with the alteration of pressure of the system for a particular temperature. The expression for the Freundlich isotherm can be represented by the following equation:

$$q_e = K_F C_e^{\frac{1}{n}} \quad (5)$$

The equation then rearranged into linear form as

$$logq_e = logK_F + (1/n)logC_e \quad (6)$$

Where, K_F = Freundlich constant.

n (gL^{-1}) = degree of the deviation from linearity of adsorption and

1/n = heterogeneity factor.

Freundlich constants at equilibrium were determined from the value of log q_e versus log C_e.

According to Temkin isotherm, most of the molecules showed lessening to heat of adsorption steadily instead of logarithmic with coverage which expressed by the following equation:

$$q_e = BlnA + BlnC_e \quad (7)$$

Here, A (mgL^{-1}) = binding constant at equilibrium linked to the binding energy at maximum level, and

B = Temkin constant.

The parameter of adsorption isotherms for JSP, MB-JSP and AMB-JSP presented in Table S1, S2 and S3 respectively. R^2 value from the Langmuir isotherm graph was nearer to 1 for both JSP and MB-JSP as compared to the values of other two isotherms. This result revealed the monolayer adsorption of MB took place by raw JSP and MB-JSP. From Langmuir adsorption isotherm q_{max} (mgg^{-1}) found 157.23 and 169.45 mgg^{-1} at 303K for both JSP and MB-JSP respectively. Multilayer adsorption took place in AMB-JSP as R^2 value was higher in Freundlich adsorption isotherms compared to other two isotherms. The main reason for multilayer formation was the alteration of the surface of raw JSP by amine crosslinked and magnetic Fe_3O_4. The maximum adsorption by AMB-JSP increased to 181.49 mgg^{-1} at 303.15K.

Removal of MeB by some raw adsorbent and modified adsorbent and their adsorption capacity was presented in Table 1. In comparison with previous work shown in the table, our prepared raw JSP and modified MB-JSP and AMB-JSP showed comparably high adsorption capacity.

Table 1. Comparison of adsorption capacity of MeB by using raw and modified adsorbent

	Adsorbent	Adsorbent isotherm	Adsorption kinetics	Adsorption capacity (mgg^{-1})	Reference
Raw	Terminalia catappa shell	Freundlich	Pseudo second order	88.62	[36]
	Grape peel	Langmuir	Pseudo second order	215.7	[37]
	Oil palm ash zeolite/chitosan	Freundlich	Pseudo second order	151.51	[38]
	Citrus sinensis	Langmuir	Pseudo second order	96.4	[38]
	Pineapple peel	Langmuir	pseudo-first-order and pseudo-second-order	97.09	[39]
	Potato peel	Langmuir	Pseudo second order	105.26	[40]
	Mango leaf powder	Langmuir	Pseudo second order	156	[41]
	Melon peel	Langmuir	Pseudo second order	333	[40]
	Bamboo shoot	Langmuir	Pseudo second order	29.88	[42]

	JSP	Langmuir	Interparticle diffusion kinetics	157.23	Present study
Modified	Corncob	Langmuir	Pseudo second order	163.93	[43]
	Corn straw core and chitosan	Langmuir	Pseudo second order	122	[44]
	Tectona grandis sawdust	Langmuir	Pseudo second order	172.41	[45]
	Coconut waste	Langmuir	Pseudo second order	138.88	[46]
	MB-JSP	Langmuir	Interparticle diffusion kinetics	169.45	Present study
	AMB-JSP	Freundlich	Interparticle diffusion kinetics	181.49	Present study

3.2.6. Kinetics of Adsorption

It is very significant to study the kinetic model for knowing the rate of interaction and dynamic behavior for the removal of MeB by means of the JSP, MB-JSP, and AMB-JSP biopolymers. The properties of dynamic adsorption were explained with the help of pseudo-first order, pseudo-second-order and intra-particle diffusion models. The ability to accept MeB (qt, mgg^{-1}) was measured by using the equation below

$$q_t = (C_O - C_t)v/m \quad (8)$$

Where, C_t= concentrations (mgL^{-1}) of MeB at time t

C_0 = concentrations (mgL^{-1}) of MeB at time 0

V = solution volume (L)and

m = adsorbents mass.

The kinetic models of MeB onto JSP, MB-JSP, and AMB-JSP were determined through the expression below:

The pseudo–first order equation is stated as

$$(q_e - q_t) = logq_e - \frac{k}{2.303t} \quad (9)$$

where, q_e (mgg^{-1}) = equilibrium adsorption

q_t (mgg^{-1}) =equilibrium adsorption and time t (min), respectively.The rate constant is k (min^{-1}).

The pseudo-second order equation can be stated as

$$t/q_t = 1/k_2q_e^2 + t/q_e \quad (10)$$

where, k_2 ($gmg^{-1}min^{-1}$) = the rate constant of the second-order equation.

q_e were obtained from intercept and slope of the plot of t/q_t vs t.

To plot the equation into intraparticle diffusion model is shown below:

$$q_t = K_{idt}^{0.5} + C \quad (11)$$

where, k_{id} ($gmg^{-1}min^{-1/2}$) = intra-particle diffusion rate constant

q_t (mgg^{-1}) = quantity of metal ion adsorbed at time t,

the intercept is C (mgg^{-1}).

The pseudo–first order, pseudo–second order and Intraparticle diffusion model of JSP, MB-JSP and AMB-JSP tentative data signified by Fig. 7, Fig. 8 and Fig. 9.

Fig 7. Pseudo – first order, pseudo – second order and Intraparticle diffusion model of JSP.

Fig 8. Pseudo – first order, pseudo – second order and Intraparticle diffusion model of MB-JSP.

Fig 9. Pseudo – first order, pseudo – second order and Intraparticle diffusion model of AMB-JSP.
The rate constant value, linear correlation coefficients (R^2), experimental (qe,exp) and (qe,cal) values for MeB shown in Table S4, S5 and S6.

3.3 Regeneration and reuse of JSP, MB-JSP and AMB-JSP

The recovery of adsorbent is very significant for lowering the process cost of adsorption and reuse for the removal of pollutants. In our study, we used three reagents: 90% ethanol, 1 $molL^{-1}$ NaOH, and 1 $molL^{-1}$ HCl. Fig.10. illustrates that the ethanol was the most effective eluent which desorbs MeB from JSP, MB-JSP and AMB-JSP. For JSP,the maximum removal percentage of MeB after cycle 3 were found to be 71.54, 64.45 and 71.22 % by using ethanol, NaOH and HCl, respectively. For MB-JSP,the maximum removal percentage of MeB after cycle 3 were found to be 71.23,71.26and 76.32% by using ethanol, NaOH and HCl, respectively. After 3 cycle, the maximum removal percentage of MeB for AMB-JSP were found to be 71.54, 64.45 and 71.22% by using ethanol, NaOH and HCl, respectively.

Fig 10. Regenration of JSP, MB-JSP and AMB-JSP by using C_2H_5OH, NaOH and HCl in three consecutive cycles

After MeB adsorption,the adsorption capacity of JSP, MB-JSP and AMB-JSP declines quickly throughout the regeneration. Because during the MeB adsorption, a huge quantity of chemical reactions happened on the JSP, MB-JSP and AMB-JSP surface and the structure of pores distorted. Due to this, the capacity of adsorption reduced significantly after regeneration[17].

4. Conclusion

The effectiveness of AMB-JSP as adsorbents for the elimination of MeB from synthetic contaminated water solution and the comparison of the adsorption parameters of JSP and MB-JSP with AMB-JSP were studied in our work. The batch mode adsorption experiments were conducted to determine the consequence of different variables such as the effect of agitation time, adsorbent dosage, initial concentration of the MeB, temperature and pH. The adsorbents such as JSP, MB-JSP and AMB-JSP were suitable to treat the wastewater containing MeB. The surface characterization of the raw and synthesized adsorbents from our study carried out by means of FESEM, XRD, FTIR and VSM gave valuable information about the high surface area, crystalline structure, functional groups and magnetic properties which were appropriate for the MeB adsorption from wastewater. The stability of adsorbents in higher temperatures found from the study of TGA and DSC of three biopolymers revealed the order as AMB-JSP>MB-JSP>JSP. We can conclude from FTIR analysis that the Fe_3O_4 nanoparticles had been effectively introduced on the raw jute stick powder surface by which MB-JSP obtained. The maximum MeB uptake for JSP, MB-JSP and AMB-JSP were found to be 157.23, 169.45 and 181.49 mgg^{-1} for JSP, MB-JSP and AMB-JSP respectively. Therefore, the maximum efficiency of MeB removal by JSP, MB-JSP and AMB-JSP were obtained at pH 6.0, 7.0 and 8.0 at 303.15 K temperature whereas the equilibrium agitation time were different as 160, 120 and 40 min for JSP, MB-JSP and AMB-JSP respectively at temperature 303.15 K. The Langmuir adsorption isotherm was suited for both JSP and MB-JSP and Freundlich isotherm was best fitted for AMB-JSP. The interparticle diffusion kinetics was the reaction kinetics for JSP, MB-JSP and AMB-JSP which showed R^2 closer to 1 compared to the pseudo-first order and pseudo-second order kinetics of MeB removal experiment. The maximum recovery of the JSP, MB-JSP and AMB-JSP biopolymers can be obtained by using 90% C_2H_5OH as compared to NaOH and HCl. From the above results, the JSP, MB-JSP and AMB-JSP can be used as excellent biopolymers for the removal of MeB from wastewater.

Acknowledgement

The authors acknowledge the research project code: CUET/DRE/2015-16/CHEM/006 of Chittagong University of Engineering & Technology, Chattogram-4349, Bangladesh.

Conflict of interest

There is no conflict of interest regarding the publication in this article.

Authors Contribution

Materials preparation, data collection, and analysis were done by Md. Masudur Rhaman, Md. Din Islam, Md. Rezaul Karim, Yunus Ahmed and M.K. Mohammad Ziaul Hyder. The first draft of manuscript was written by Md. Masudur Rhaman and Md. Din Islam. All authors read and approved the final manuscript.

Data availability statement

Source data for all figures and tables are provided with the paper and available with articles.

References:

1. Bhateria R, Jain D (2016) Water quality assessment of lake water: a review. Sustain. Water Resour. Manag. 2:161–173. https://doi.org/10.1007/s40899-015-0014-7

2. Hyder MKMZ, Mir SH (2021) Performance of Metal-Based Nanoparticles and Nanocomposites for Water Decontamination. In: Eric L, Ali K, Subramanian, S. M. (eds) Inorganic-Organic Composites for Water and Wastewater Treatment, 1st ed. pp 65–112

3. Selvaraj V, Swarna Karthika T, Mansiya C, Alagar M (2021) An over review on recently developed techniques, mechanisms and intermediate involved in the advanced azo dye degradation for industrial applications. J. Mol. Struct. 1224:. https://doi.org/10.1016/j.molstruc.2020.129195

4. Miyah Y, Lahrichi A, Idrissi M (2016) Removal of cationic dye -Methylene bleu- from aqueous solution by adsorption onto corn cob powder calcined. J. Mater. Environ. Sci. 7:96–104

5. Tuli FJ, Hossain A, Kibria AKMF, Tareq ARM, Mamun SMMA, Ullah AKMA (2020) Removal of methylene blue from water by low-cost activated carbon prepared from tea waste: A study of adsorption isotherm and kinetics. Environ. Nanotechnol. Monit. Manag. 14:100354. https://doi.org/10.1016/j.enmm.2020.100354

6. Khan TA, Khan EA, Shahjahan (2016) Adsorptive uptake of basic dyes from aqueous solution by novel brown linseed deoiled cake activated carbon: Equilibrium isotherms and dynamics. J. Environ. Chem. Eng. 4:3084–3095. https://doi.org/10.1016/j.jece.2016.06.009

7. Javaid R, Qazi UY (2019) Catalytic oxidation process for the degradation of synthetic dyes: An overview. Int. J. Environ. Res. 16:1–27. https://doi.org/10.3390/ijerph16112066

8. Yadav V, Ali J, Garg MC (2021) Biosorption of Methylene Blue Dye from Textile-Industry Wastewater onto Sugarcane Bagasse: Response Surface Modeling, Isotherms, Kinetic and Thermodynamic Modeling. J. Hazard. Toxic Radioact. Waste 25:04020067. https://doi.org/10.1061/(asce)hz.2153-5515.0000572

9. Hyder MKMZ, Ochiai B (2017) Synthesis of a Selective Scavenger for Ag(I), Pd(II), and Au(III) Based on Cellulose Filter Paper Grafted with Polymer Chains Bearing Thiocarbamate Moieties. Chem. Lett. 46:492–494. https://doi.org/10.1246/cl.160983

10. Aryee AA, Mpatani FM, Kani AN, Dovi E, Han R, Li Z, Qu L (2020) Iminodiacetic acid functionalized magnetic peanut husk for the removal of methylene blue from solution: characterization and equilibrium studies. Environ. Sci. Pollut. Res. 27:40316–40330. https://doi.org/10.1007/s11356-020-10087-6

11. Hameed BH, Ahmad AA (2009) Batch adsorption of methylene blue from aqueous solution by garlic peel, an agricultural waste biomass. J.Hazard.Mater. 164:870–875. https://doi.org/10.1016/j.jhazmat.2008.08.084

12. Ghosh I, Kar S, Chatterjee T, Bar N, Das SK (2021) Removal of methylene blue from aqueous solution using Lathyrus sativus husk: Adsorption study, MPR and ANN modelling. Process Saf. Environ. Prot.149:345–361. https://doi.org/10.1016/j.psep.2020.11.003

13. Mahamad MN, Zaini MAA, Zakaria ZA (2015) Preparation and characterization of activated carbon from pineapple waste biomass for dye removal. Int. Biodeterior. Biodegradation 102:274–280. https://doi.org/10.1016/j.ibiod.2015.03.009

14. Wu L, Zhang X, Anthony Thorpe J, Li L, Si Y (2020) Mussel-inspired polydopamine functionalized recyclable coconut shell derived carbon nanocomposites for efficient adsorption of methylene blue. J. Saudi Chem. Soc. 24:642–649. https://doi.org/10.1016/j.jscs.2020.07.002

15. Krishna Murthy TP, Gowrishankar BS, Krishna RH, Chandraprabha MN, Mathew BB (2020) Magnetic modification of coffee husk hydrochar for adsorptive removal of methylene blue: Isotherms, kinetics and thermodynamic studies. Environ. Chem. Ecotoxicol. 2:205–212. https://doi.org/10.1016/j.enceco.2020.10.002

16. Tran TH, Le AH, Pham TH, Nguyen DT, Chang SW, Chung WJ, Nguyen DD (2020) Adsorption isotherms and kinetic modeling of methylene blue dye onto a carbonaceous hydrochar adsorbent derived from coffee husk waste. Sci.Total Environ. 725:138325. https://doi.org/10.1016/j.scitotenv.2020.138325

17. Li H, Liu L, Cui J, Cui J, Wang F, Zhang F (2020) High-efficiency adsorption and regeneration of methylene blue and aniline onto activated carbon from waste edible fungus residue and its possible mechanism. RSC Advances 10:14262–14273. https://doi.org/10.1039/d0ra01245a

18. Ahmad A, Khan N, Giri BS, Chowdhary P, Chaturvedi P (2020) Removal of methylene blue dye using rice husk, cow dung and sludge biochar: Characterization, application, and kinetic studies. Bioresour. Technol. 306:123202. https://doi.org/10.1016/j.biortech.2020.123202

19. Alver E, Metin AÜ, Brouers F (2020) Methylene blue adsorption on magnetic alginate/rice husk bio-composite. Int. J. Biol. Macromol. 154:104–113. https://doi.org/10.1016/j.ijbiomac.2020.02.330

20. Bayomie OS, Kandeel H, Shoeib T, Yang H, Youssef N, El-Sayed MMH (2020) Novel approach for effective removal of methylene blue dye from water using fava bean peel waste. Sci. Rep. 10:1–10. https://doi.org/10.1038/s41598-020-64727-5

21. Cusioli LF, Quesada HB, Baptista ATA, Gomes RG, Bergamasco R (2020) Soybean hulls as a low-cost biosorbent for removal of methylene blue contaminant. Environ. Prog. Sustain. Energy 39:. https://doi.org/10.1002/ep.13328

22. Esa YAM, Sapawe N (2020) Removal of methylene blue from aqueous solution using silica nanoparticle extracted from skewer coconut leaves. Mater. Today: Proceedings 31:398–401. https://doi.org/10.1016/j.matpr.2020.07.192

23. Francis AO, Zaini MAA, Muhammad IM, Abdulsalam S, El-Nafaty UA (2020) Adsorption dynamics of dye onto crab shell chitosan/neem leaf composite. Water Pract. Technol. 15:673–682. https://doi.org/10.2166/wpt.2020.054

24. Patel H, Vashi RT (2013) A comparison study of removal of methylene blue dye by adsorption on Neem leaf powder (NLP) and activated NLP. J. Environ. Eng. Landsc. Manag. 21:36–41. https://doi.org/10.3846/16486897.2012.671772

25. Sen TK, Afroze S, Ang HM (2011) Equilibrium, kinetics and mechanism of removal of methylene blue from aqueous solution by adsorption onto pine cone biomass of Pinus radiata. Water Air Soil Pollut. 218:499–515. https://doi.org/10.1007/s11270-010-0663-y

26. Maia LS, da Silva AIC, Carneiro ES, Monticelli FM, Pinhati FR, Mulinari DR (2021) Activated Carbon From Palm Fibres Used as an Adsorbent for Methylene Blue Removal. J. Polym. Environ. 29:1162–1175. https://doi.org/10.1007/s10924-020-01951-0

27. Bhadusha N, Ananthabaskaran T (2011) Adsorptive removal of methylene blue onto ZnCl2 activated carbon from wood apple outer shell: Kinetics and equilibrium studies. E. J. Chem. 8:1696–1707. https://doi.org/10.1155/2011/429831

28. Qian WC, Luo XP, Wang X, Guo M, Li B (2018) Removal of methylene blue from aqueous solution by modified bamboo hydrochar. Ecotoxicol. Environ. Saf. 157:300–306. https://doi.org/10.1016/j.ecoenv.2018.03.088

29. Tzy SJ, Cheah YY, Peck LK, Shi Jong T, Yong Yoo C, Loo Kiew P (2020) Feasibility study of methylene blue adsorption using magnetized papaya seeds. Prog. Energy Environ. 14:1–12

30. Hyder MKMZ, Ochiai B (2018) Selective recovery of Au(III), Pd(II), and Ag(I) from printed circuit boards using cellulose filter paper grafted with polymer chains bearing thiocarbamate moieties. Microsyst. Technol. 24:683–690. https://doi.org/10.1007/s00542-017-3277-0

31. Senthilkumaar S, Varadarajan PR, Porkodi K, Subbhuraam C V. (2005) Adsorption of methylene blue onto jute fiber carbon: Kinetics and equilibrium studies. J. Colloid Interface Sci. 284:78–82. https://doi.org/10.1016/j.jcis.2004.09.027

32. Chakraborty TK, Islam MS, Zaman S, Kabir AHME, Ghosh GC (2020) Jute (Corchorus olitorius) stick charcoal as a low-cost adsorbent for the removal of methylene blue dye from aqueous solution. SN Appl. Sci. 2:. https://doi.org/10.1007/s42452-020-2565-y

33. Rhaman MM, Karim MR, Hyder MKMZ, Ahmed Y, Nath RK (2020) Removal of Chromium (VI) from Effluent by a Magnetic Bioadsorbent Based on Jute Stick Powder and its Adsorption Isotherm, Kinetics and Regeneration Study. Water Air Soil Pollut. 231:. https://doi.org/10.1007/s11270-020-04544-8

34. Song W, Gao B, Xu X, Wang F, Xue N, Sun S, Song W, Jia R (2016) Adsorption of nitrate from aqueous solution by magnetic amine-crosslinked biopolymer based corn stalk and its chemical regeneration property. J. Hazard. Mater. 304:280–290. https://doi.org/10.1016/j.jhazmat.2015.10.073

35. Hyder MKMZ, Ochiai B (2022) Synthesis of a Highly Selective Scavenger of Precious Metals from a Printed Circuit Board Based on Cellulose Filter Paper Functionalized with a Grafted Polymer Chain Bearing N -Methyl-2-hydroxyethylcarbamothioate Moieties. ACS Omega 7:10355–10364. https://doi.org/10.1021/acsomega.1c06988

36. Hevira L, Zilfa, Rahmayeni, Ighalo JO, Aziz H, Zein R (2021) Terminalia catappa shell as low-cost biosorbent for the removal of methylene blue from aqueous solutions. J. Ind. Eng. Chem. 97:188–199. https://doi.org/10.1016/j.jiec.2021.01.028

37. Ma L, Jiang C, Lin Z, Zou Z (2018) Microwave-hydrothermal treated grape peel as an efficient biosorbent for methylene blue removal. Int. J. Environ. Res. 15:. https://doi.org/10.3390/ijerph15020239

38. Khanday WA, Asif M, Hameed BH (2017) Cross-linked beads of activated oil palm ash zeolite/chitosan composite as a bio-adsorbent for the removal of methylene blue and acid blue 29 dyes. International Journal of Biological Macromol. 95:895–902. https://doi.org/10.1016/j.ijbiomac.2016.10.075

39. Krishni RR, Foo KY, Hameed BH (2014) Food cannery effluent, pineapple peel as an effective low-cost biosorbent for removing cationic dye from aqueous solutions. Desalination Water Treat. 52:6096–6103. https://doi.org/10.1080/19443994.2013.815686

40. Djelloul C, Hamdaoui O (2014) Removal of cationic dye from aqueous solution using melon peel as nonconventional low-cost sorbent. Desalination Water Treat. 52:7701–7710. https://doi.org/10.1080/19443994.2013.833555

41. Uddin MdT, Rahman MdA, Rukanuzzaman Md, Islam MdA (2017) A potential low cost adsorbent for the removal of cationic dyes from aqueous solutions. Appl. Water Sci. 7:2831–2842. https://doi.org/10.1007/s13201-017-0542-4

42. Zhu L, Zhu P, You L, Li S (2019) Bamboo shoot skin: turning waste to a valuable adsorbent for the removal of cationic dye from aqueous solution. Clean Technol. Environ. Policy 21:81–92. https://doi.org/10.1007/s10098-018-1617-0

43. Ma H, Li JB, Liu WW, Miao M, Cheng BJ, Zhu SW (2015) Novel synthesis of a versatile magnetic adsorbent derived from corncob for dye removal. Bioresour. Technolol 190:13–20. https://doi.org/10.1016/j.biortech.2015.04.048

44. Liu S, Ge H, Cheng S, Zou Y (2020) Green synthesis of magnetic 3D bio-adsorbent by corn straw core and chitosan for methylene blue removal. Environ. Technol. 41:2109–2121. https://doi.org/10.1080/09593330.2018.1556345

45. Bortoluz J, Ferrarini F, Bonetto LR, da Silva Crespo J, Giovanela M (2020) Use of low-cost natural waste from the furniture industry for the removal of methylene blue by adsorption: isotherms, kinetics and thermodynamics. Cellulose 27:6445–6466. https://doi.org/10.1007/s10570-020-03254-y

46. Kocaman S (2020) Synthesis and cationic dye biosorption properties of a novel low-cost adsorbent: coconut waste modified with acrylic and polyacrylic acids. Int. J. Phytoremediation 22:551–566. https://doi.org/10.1080/15226514.2020.1741509

Figures

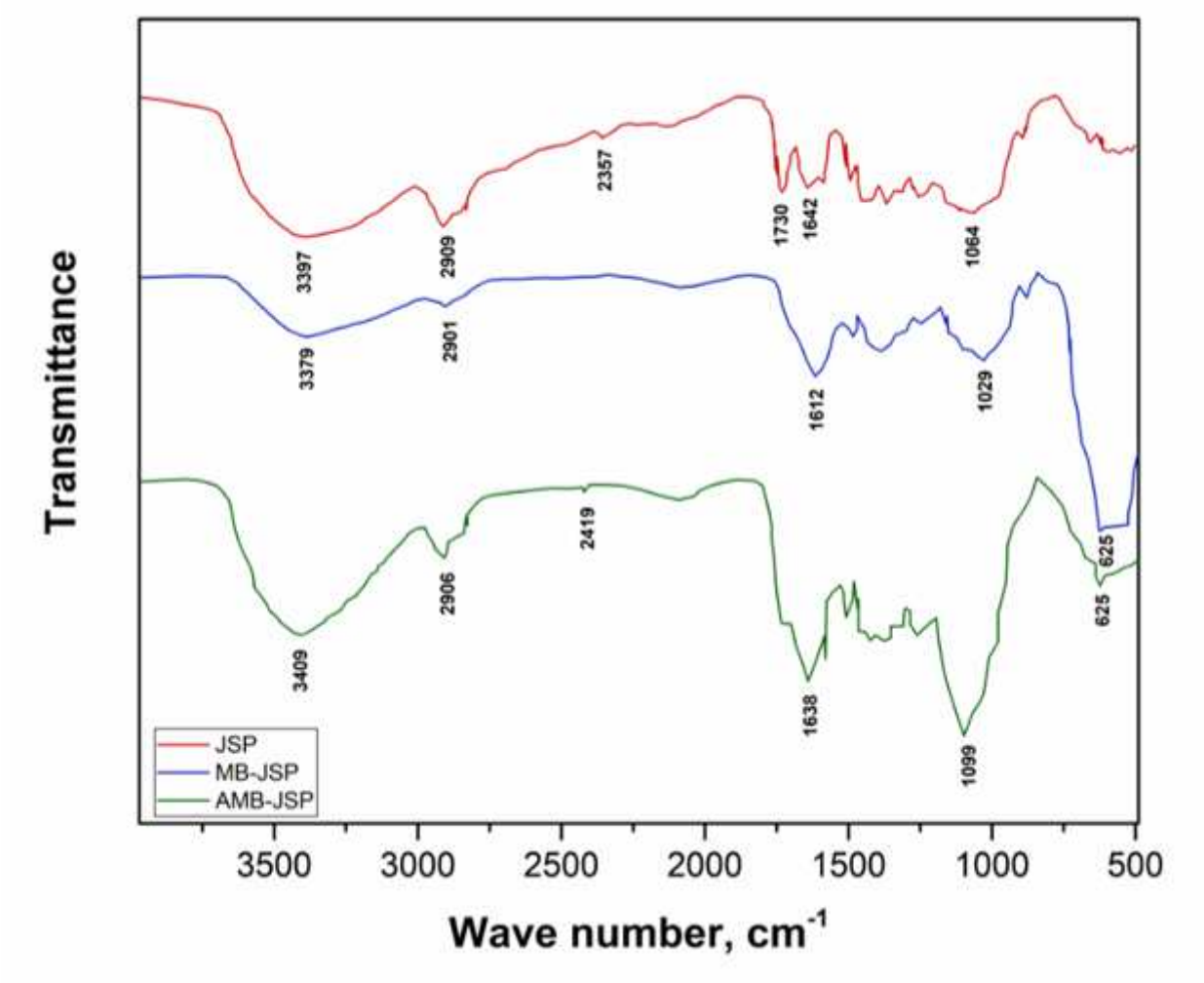

Figure 1

FTIR spectra of JSP, MB-JSP & AMB-JSP before the MeB adsorption

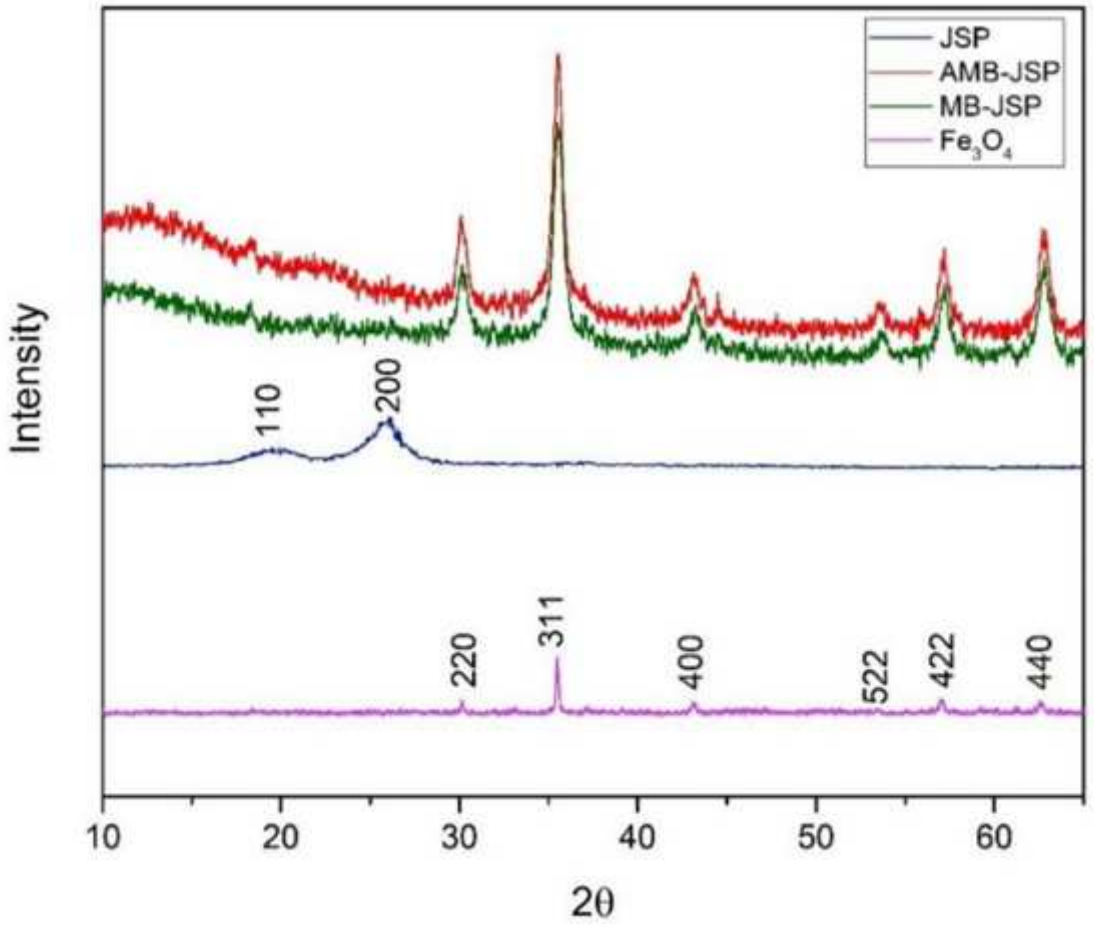

Figure 2

XRD pattern study for the identification of crystalline structures of JSP, AMB-JSP, MB-JSP and Fe_3O_4

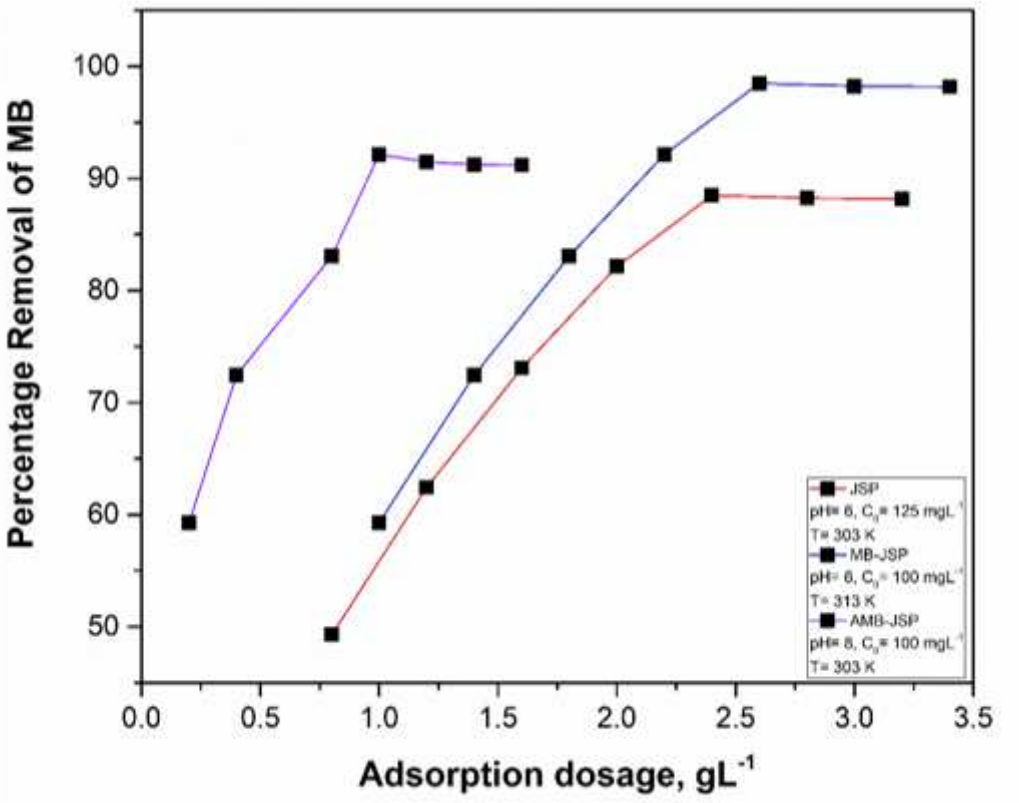

Figure 3

The effect of pH on MeB removal by JSP, MB-JSP and AMB-JSP

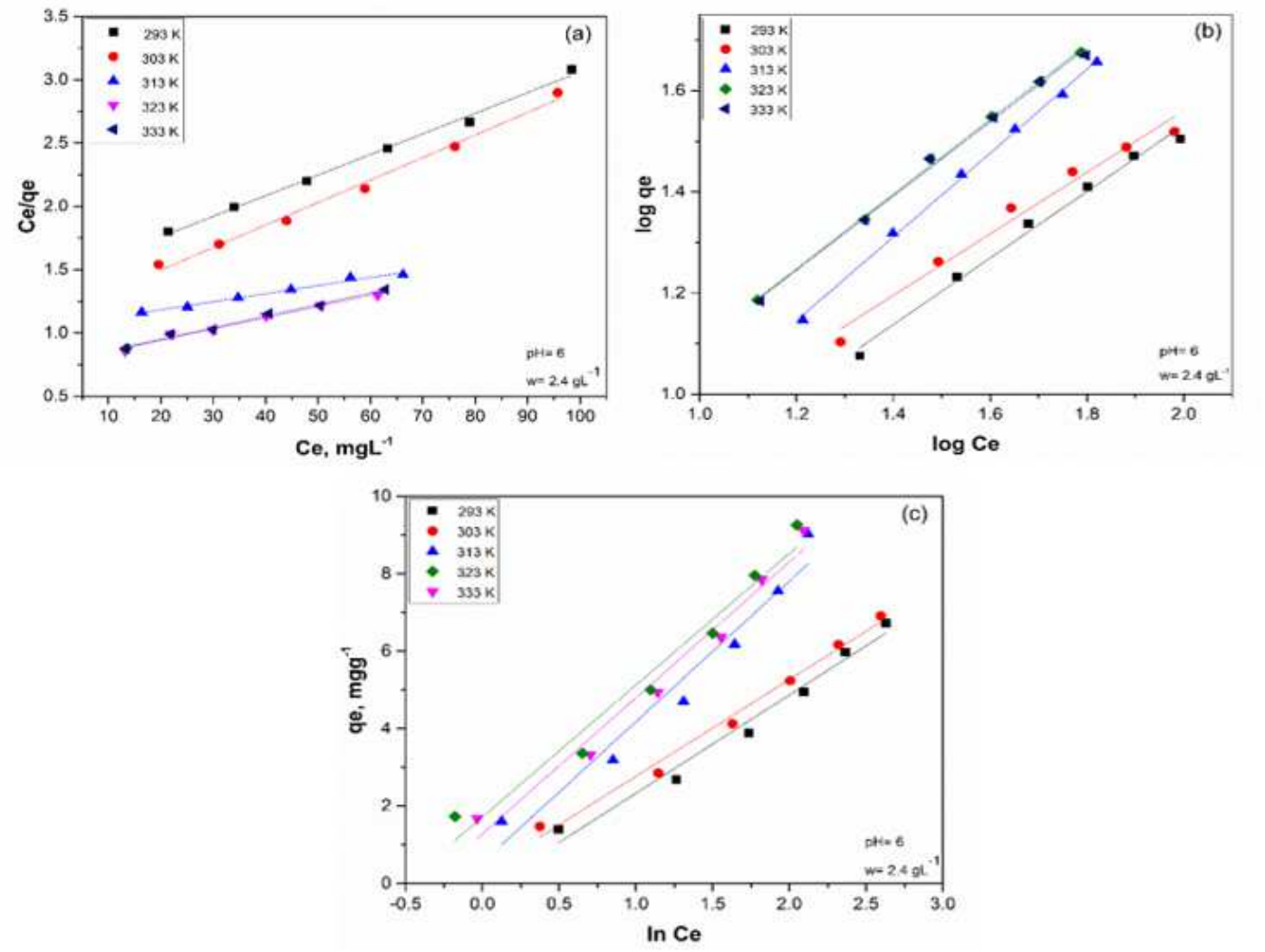

Figure 4

(a), (b) & (c) represents Langmuir, Freundlich and Temkin models respectively for the MeB removal by JSP

Figure 5

(a), (b) & (c) represents Langmuir, Freundlich and Temkin models respectively for the MeB removal by MB-JSP

Figure 6

(a), (b) & (c) represents Langmuir, Freundlich and Temkin models respectively for the MeB removal by AMB-JSP

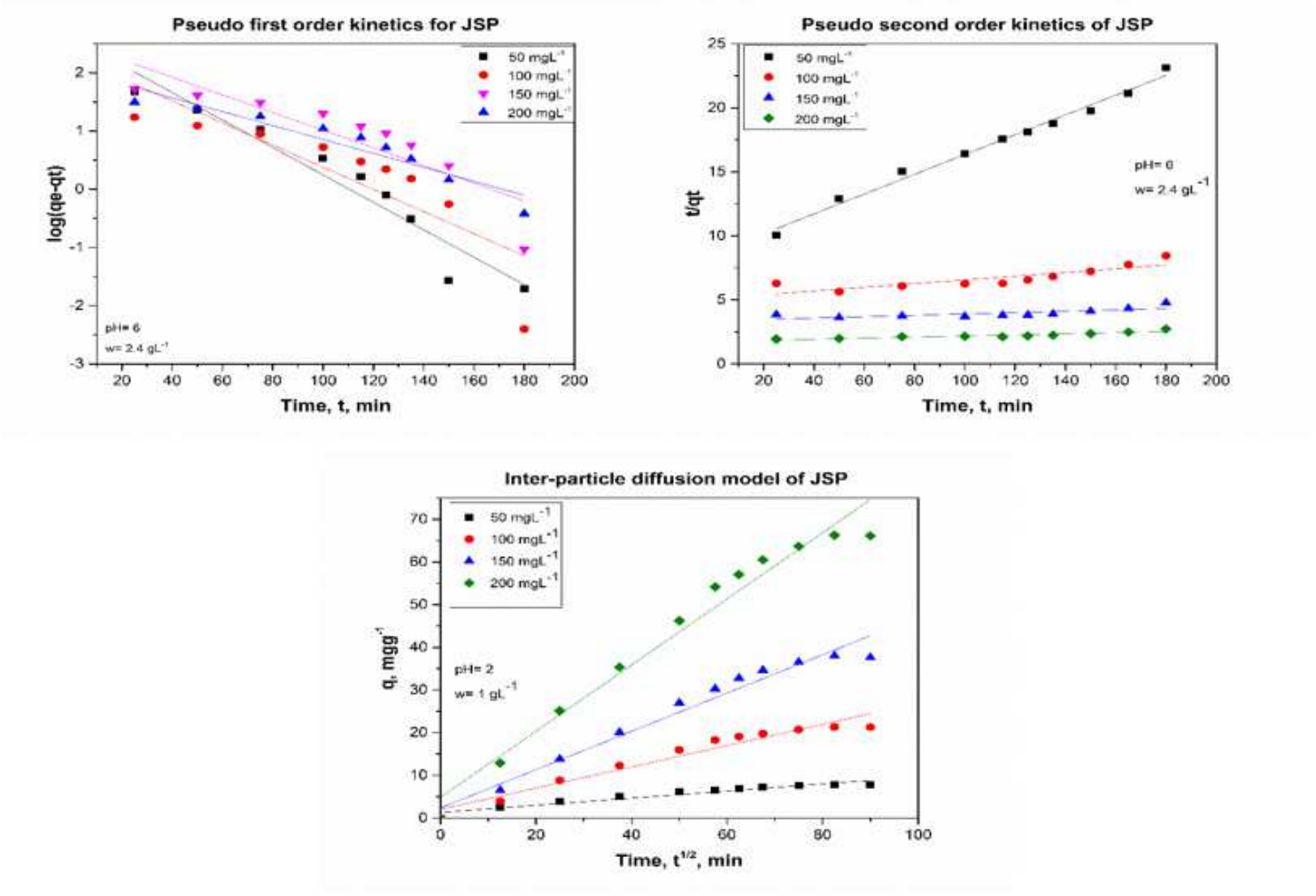

Figure 7

Pseudo – first order, pseudo – second order and Intraparticle diffusion model of JSP.

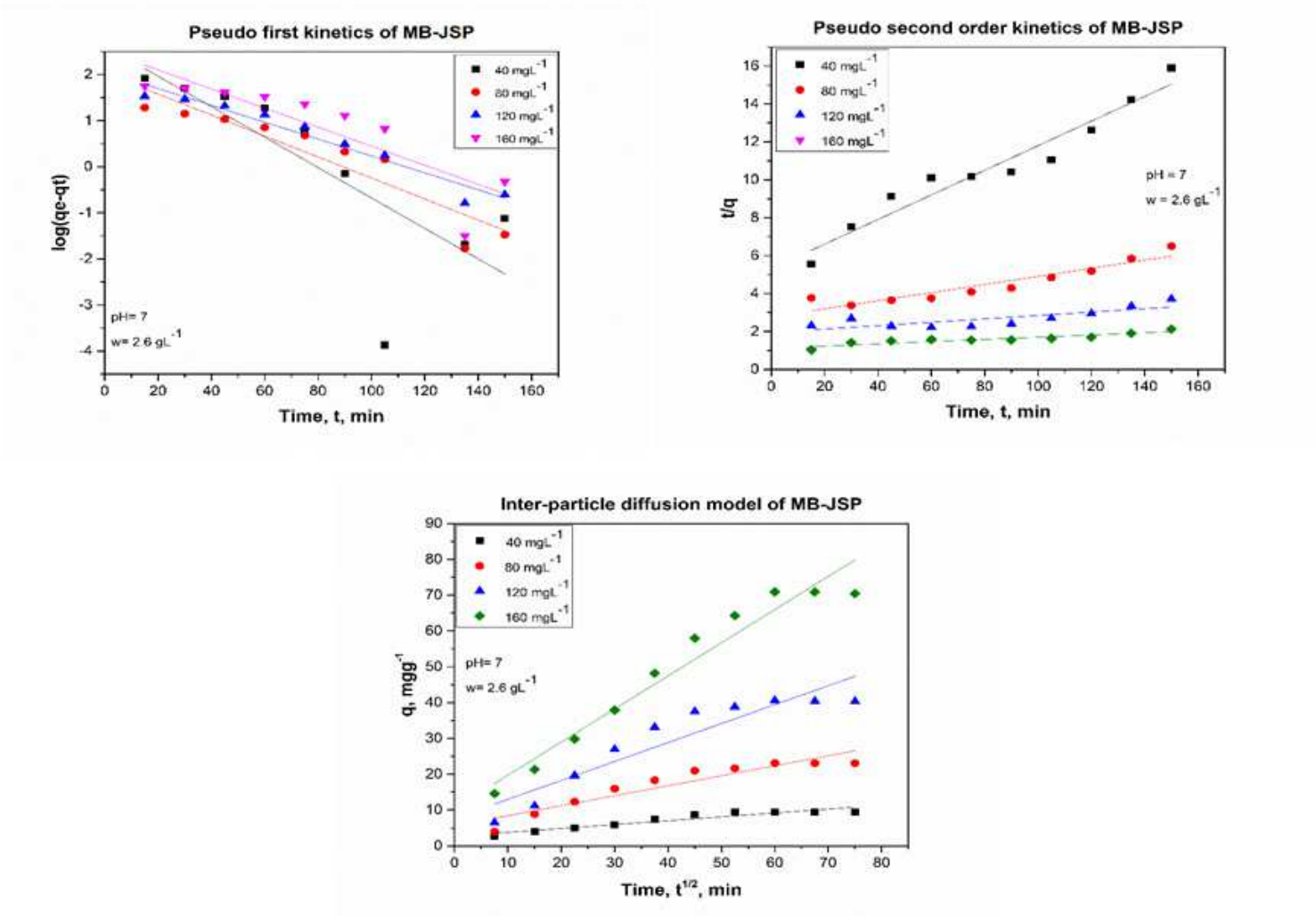

Figure 8

Pseudo – first order, pseudo – second order and Intraparticle diffusion model of MB-JSP.

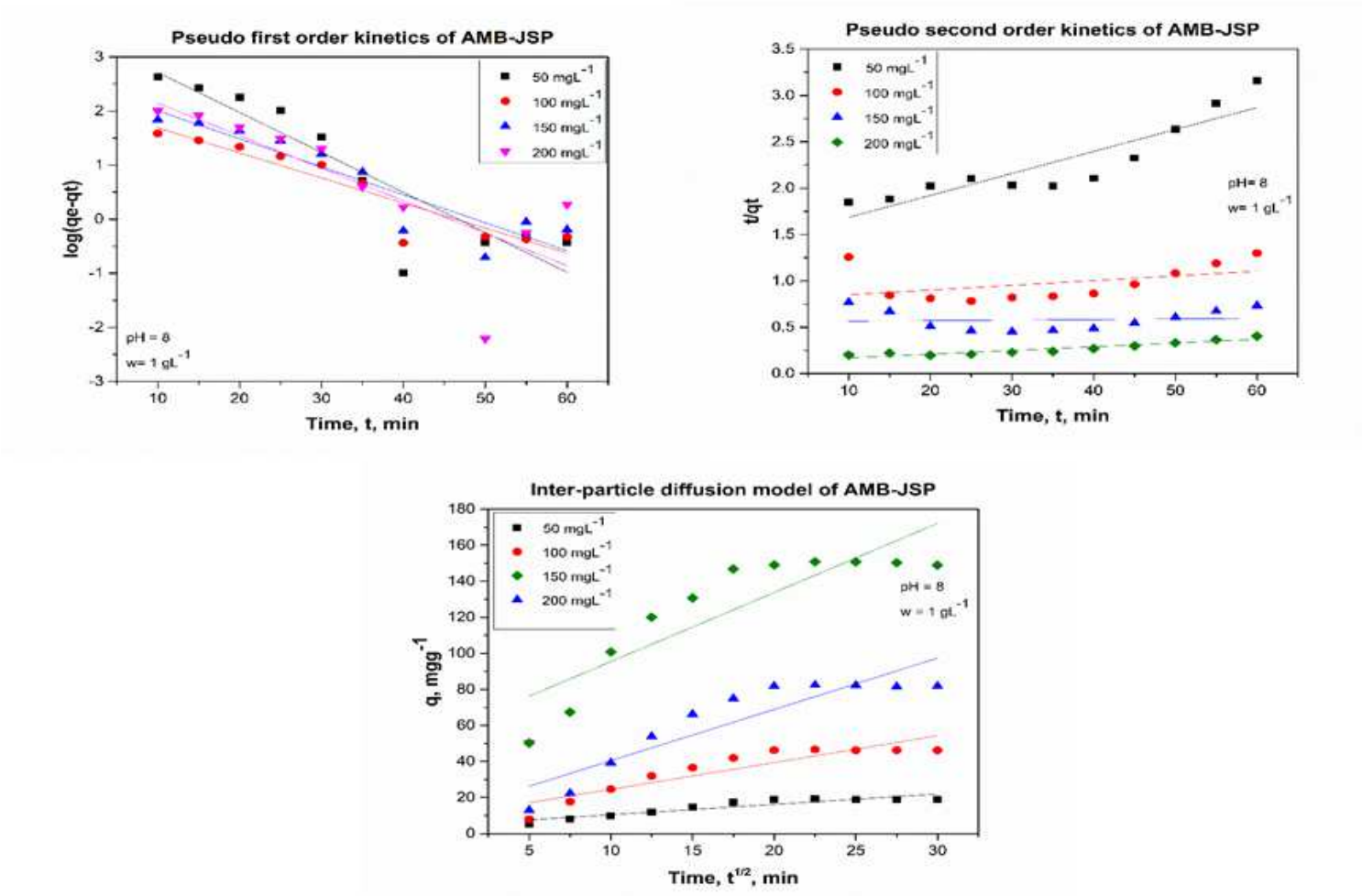

Figure 9

Pseudo – first order, pseudo – second order and Intraparticle diffusion model of AMB-JSP.

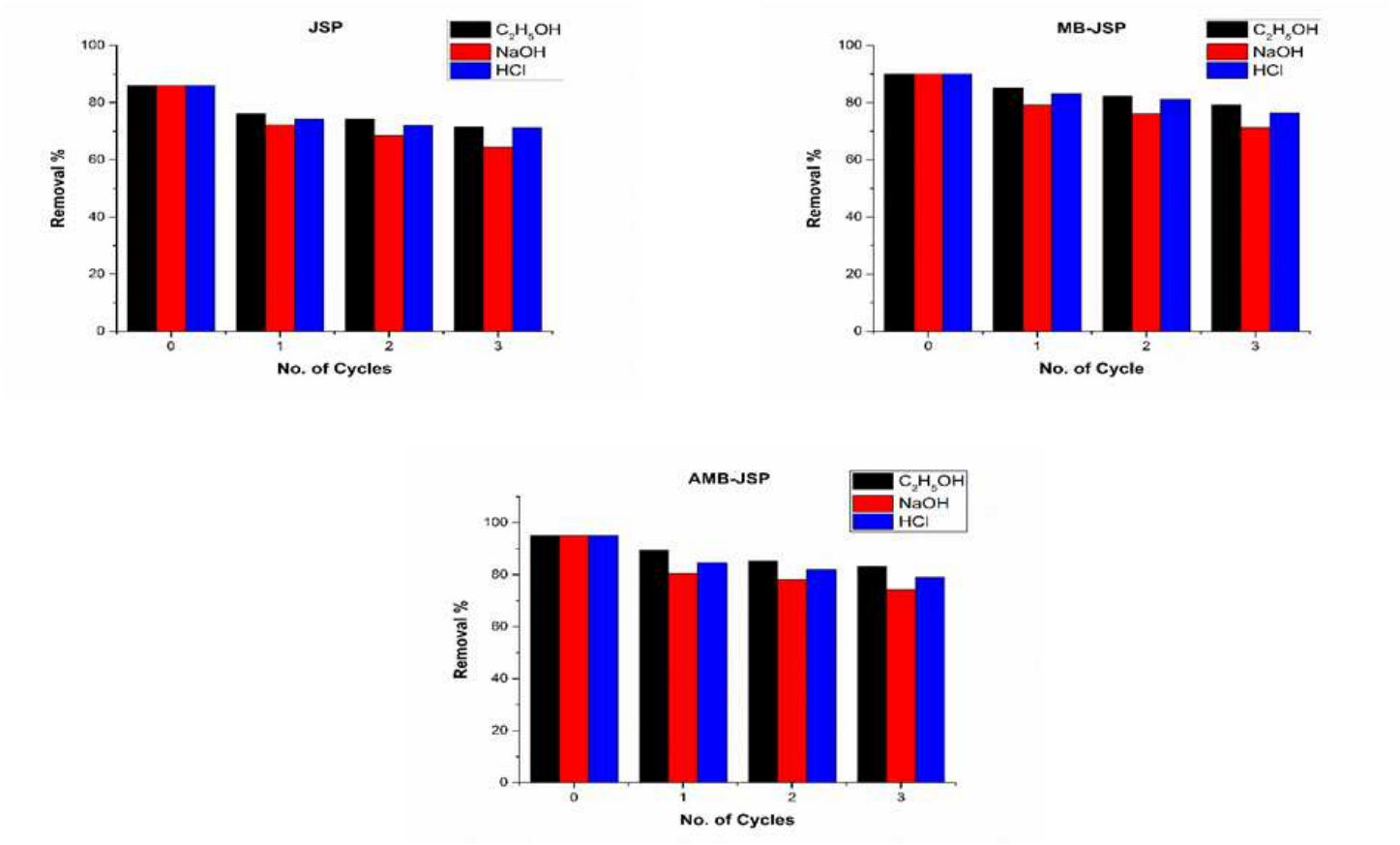

Figure 10

Regenration of JSP, MB-JSP and AMB-JSP by using C_2H_5OH, NaOH and HCl in three consecutive cycles

Supplementary Files

This is a list of supplementary files associated with this preprint. Click to download.

- Supplimentaryfile.docx